

## Supplemental Figure Legends

### **Supplemental Figure 1. ZO-1 localizes specifically to nephrocyte SDs.**

(A) Airy-scan imaging of WT nephrocytes stained with anti-ZO-1 antibody shows that ZO-1 is specifically localized to the curvilinear SDs that cover the surface of normal nephrocytes. (A') Cropped view of the region from (A) marked by the 1 $\mu$ m scale bar, which spans approximately four SDs. (B) TEM imaging confirms that SDs are spaced approximately 200-250nm apart.

### **Supplemental Figure 2. Dlg1, but not Dlg5, is required for correct localization of ZO-1 and Nephrin.**

(A) Control nephrocyte has normal surface enrichment of ZO-1 (green). (B) Animals heterozygous for both *Sns-Gal4* and *Dlg* RNAi transgenes have significantly reduced surface ZO-1 (red dashed line outlines cell boundaries). (C) This phenotype is significantly increased in animals homozygous for both the *Gal4* and RNAi transgenes. (D) Quantification of ZO-1 localization in these animals. (E) A different *Dlg* RNAi (#33620) line causes similar defects as those observed using the primary RNAi line of this study (#36771). (F) Nephrocytes from flies harboring a temperature-sensitive mutation in *dlg* and raised at the restrictive temperature of 29C show severe defects in ZO-1 localization. (G) KD of fly *Dlg5* has no appreciable effect on ZO-1 localization. (H) Similar to ZO-1 and *Neph1* (see Fig.2) the fly *Nephrin* homolog localizes to the surface of nephrocytes. (I) In *Dlg* KD cells, *Nephrin* is also mislocalized from the cell surface and into internal aggregations. Scale bars=10 $\mu$ m.

### **Supplemental Figure 3. Cytoplasmic aggregates of Dlg and Lgl do not colocalize with the ER, Golgi, or Par3.**

(A) *Lgl* (red) and *Dlg* (blue) can colocalize at cytoplasmic "clouds" in control nephrocytes, but this does not overlap with a Golgi:eYFP marker (green). (B) Similarly, the cytoplasmic aggregations of *Lgl* (red) and *Dlg* (blue) does not colocalize with an ER:eYFP marker (green). (C) We also did not observe significant enrichment of *Par3* (red) at *Dlg* clouds (green). Scale bars=10 $\mu$ m.

### **Supplemental Figure 4. Dlg and Par-1 promote normal Crb localization and protein levels.**

(A) In control nephrocytes (*Dot-Gal4* alone), *Crb* is enriched near the cell periphery. (B) In *Dlg* KD cells, *Crb* is mislocalized into cytoplasmic aggregates of varying sizes, including several large puncta (green arrows). (C) In *Par-1* KD cells, *Crb* is also mislocalized, however it is found in many small puncta spread more evenly distributed in size. (D) Quantification of *Crb* fluorescence intensity reveals a reduction in mean levels of *Crb* in both *Dlg* KD and *Par-1* KD cells. This effect appears more severe in *Dlg* KD compared to *Par-1* KD. Scale bars=10 $\mu$ m.

### **Supplemental Figure 5. Mislocalized ZO-1 in Dlg KD cells does not accumulate in the ER or Golgi, but their organization is perturbed by loss of Dlg, Nephrin, or Neph1.**

(A) In WT nephrocytes, the ER marker *Sec61B:tdTomato* (red) appears as a homogenous cloud surrounding the nuclei in the center of the cell, while the Golgi marker *Golgin84* (green) reveals punctate structures interspersed along the outer edge of the ER. (B) In *Dlg* KD cells, mislocalized ZO-1 (red) does not colocalize with the Golgi (green), however, the Golgi organization is severely disrupted in these cells; compare B' to A'. (C) While mislocalized ZO-1 (green) is also not present in the ER, the ER itself is disrupted in *Dlg* KD cells, appearing fragmented through the cytoplasm with uneven concentrations of the ER marker *Sec61B* (red); compare C'' to A''. (D) Aberrant Golgi

organization was also observed in cells depleted of Neph1. Similarly, the ER appears abnormal in cells depleted of Neph1 (E) or Neph1 (F). Scale bars=10µm.

**Supplemental Figure 6. In Dlg KD nephrocytes, mislocalized ZO-1 does not colocalize with Rab7 or Rab11, despite their aberrant subcellular distributions.**

(A) A subcortical slice of WT nephrocytes shows numerous Rab7-positive vesicles and larger circular structures (yellow arrows), which are likely late endosomes, lysosomes, and α-vacuoles (Rab7 in green; ZO-1 in red)<sup>65</sup>. (B) A medial cross-section of a WT cell indicates that the majority of Rab7-vesicles are located in the subcortical region of the cell. (C-D) In Dlg KD cells, subcortical and medial sections reveal an even distribution of Rab7 structures throughout the cell, and lack the larger circular Rab7 structures. Note that the mislocalized ZO-1 protein does not colocalize with Rab7 in Dlg KD cells. (E) WT nephrocytes show cortical enrichment of Rab11 vesicles (green), just interior to the ZO-1 positive SD region (red). (F) In Dlg KD cells, Rab11 localization is diffuse through the cytoplasm and does not colocalize with internally mislocalized ZO-1 aggregations. Scale bars=10µm.

**Supplemental Figure 7. Endocytic markers Rab7 and Rab11 are not specifically enriched in the aberrant ZO-1 aggregations caused by Par-1 KD.**

(A) The "cloud" of mislocalized SD protein ZO-1 (red) that is typical of Par-1 KD contains some Rab7 structures (green). However, in contrast to Rab5 (see Fig.5D,E), Rab7 structures do not preferentially aggregate at these sites—they appear evenly distributed throughout the cytoplasm. (B) Similarly, although Rab11 (green) can be detected in the ZO-1 aggregations in Par-1 KD, this does not appear to be a specific recruitment to that site, as seen with Rab5. Note that the more uniform distribution of Rab7 and Rab11 in Par-1 KD is qualitatively different from WT nephrocytes (compare to Suppl.Fig.6B',E'). Scale bars=10µm.

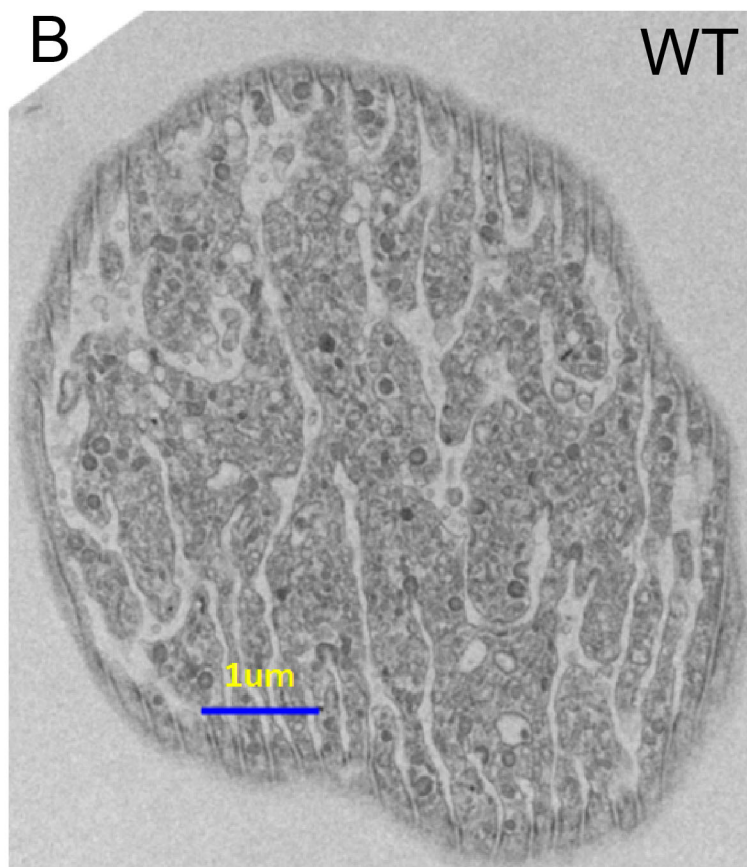
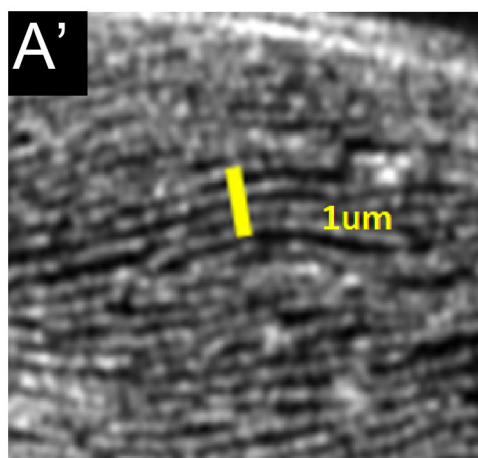
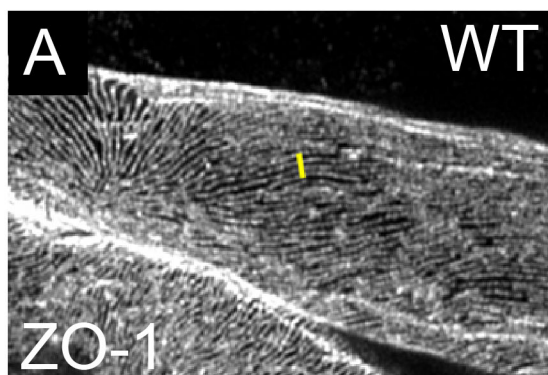
**Supplemental Figure 8. In nephrocytes depleted of Dlg or Par-1, mislocalized Neph1 and Neph1 are adjacent to Rab5 structures, while only loosely associated with Rab11 and Rab7.**

(A) In Dlg KD cells, Neph1 is mislocalized to cytoplasmic aggregates (yellow arrows), which are intermixed with mislocalized Rab5. (B) Similarly, in Par-1 KD cells, Neph1 puncta are tightly associated with dense accumulations of Rab5 vesicles, though they do not appear to colocalize. (C) Dlg KD causes a uniform disruption of Rab11 distribution, which can contain mislocalized Neph1, though again there is no colocalization or specific association of the two proteins. (D) Similar results were observed in Par-1 KD. (E) In Dlg KD, mislocalized Rab7 and Neph1 are both mislocalized, but not significantly associated with one another.

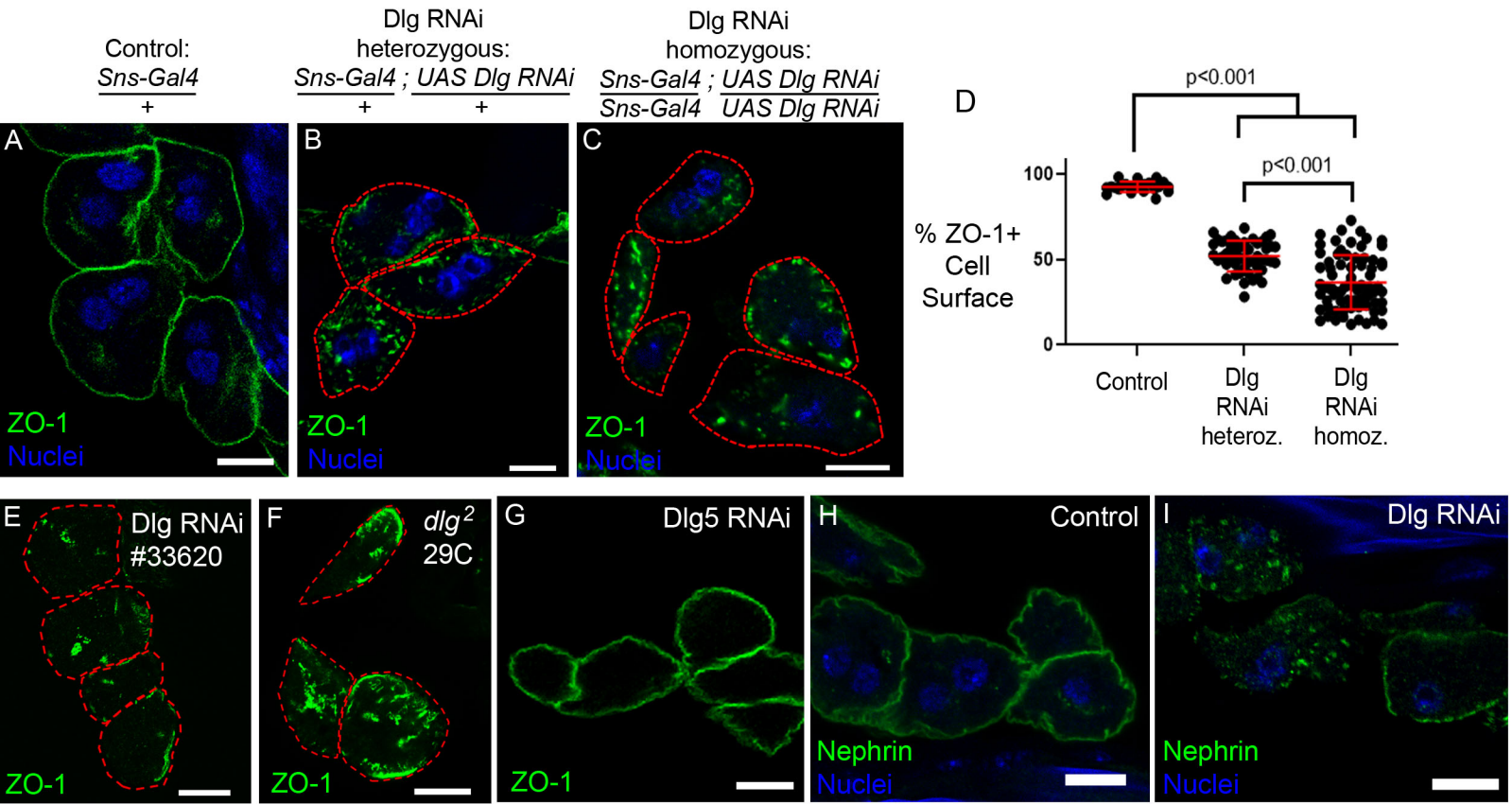
**Supplemental Figure 9. Scrib is required for normal rates of endocytosis.**

(A) Wildtype nephrocytes readily internalize 10kD fluorescent dextran. (B) Nephrocytes null mutant for *scrib* have significantly reduced dextran uptake. (C) Quantification of dextran signal shows significantly reduced fluorescence intensity in *scrib* mutant cells. Scale bars=10µm.

## Suppl.Fig.1

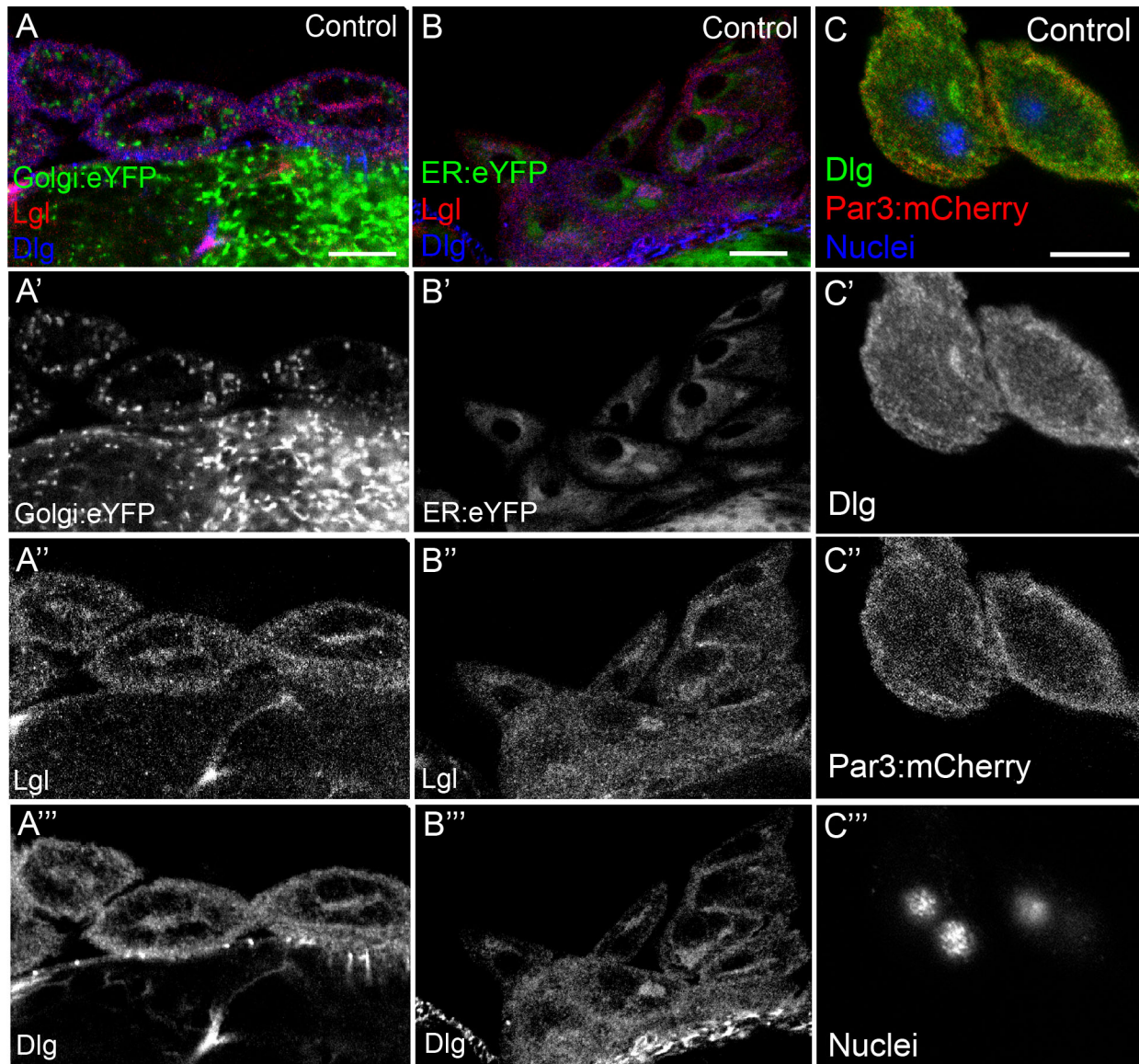


Suppl.Fig.2

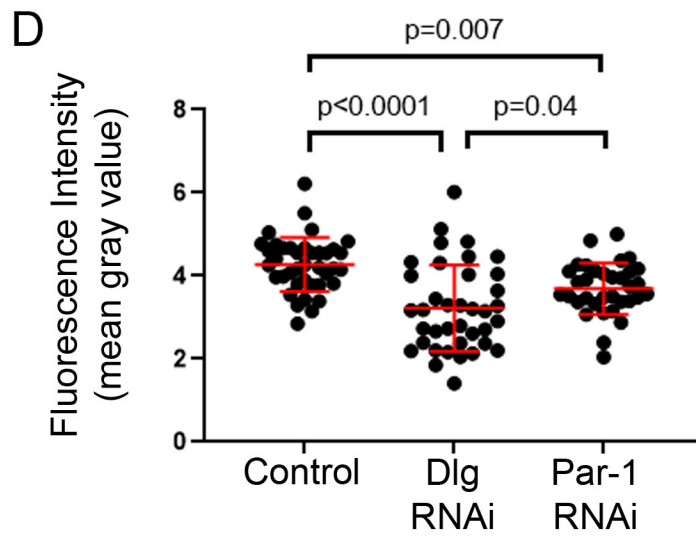
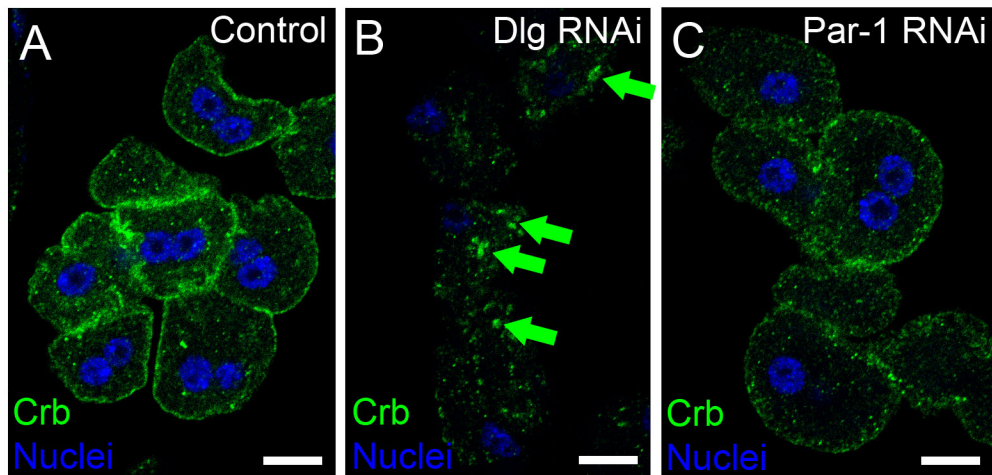




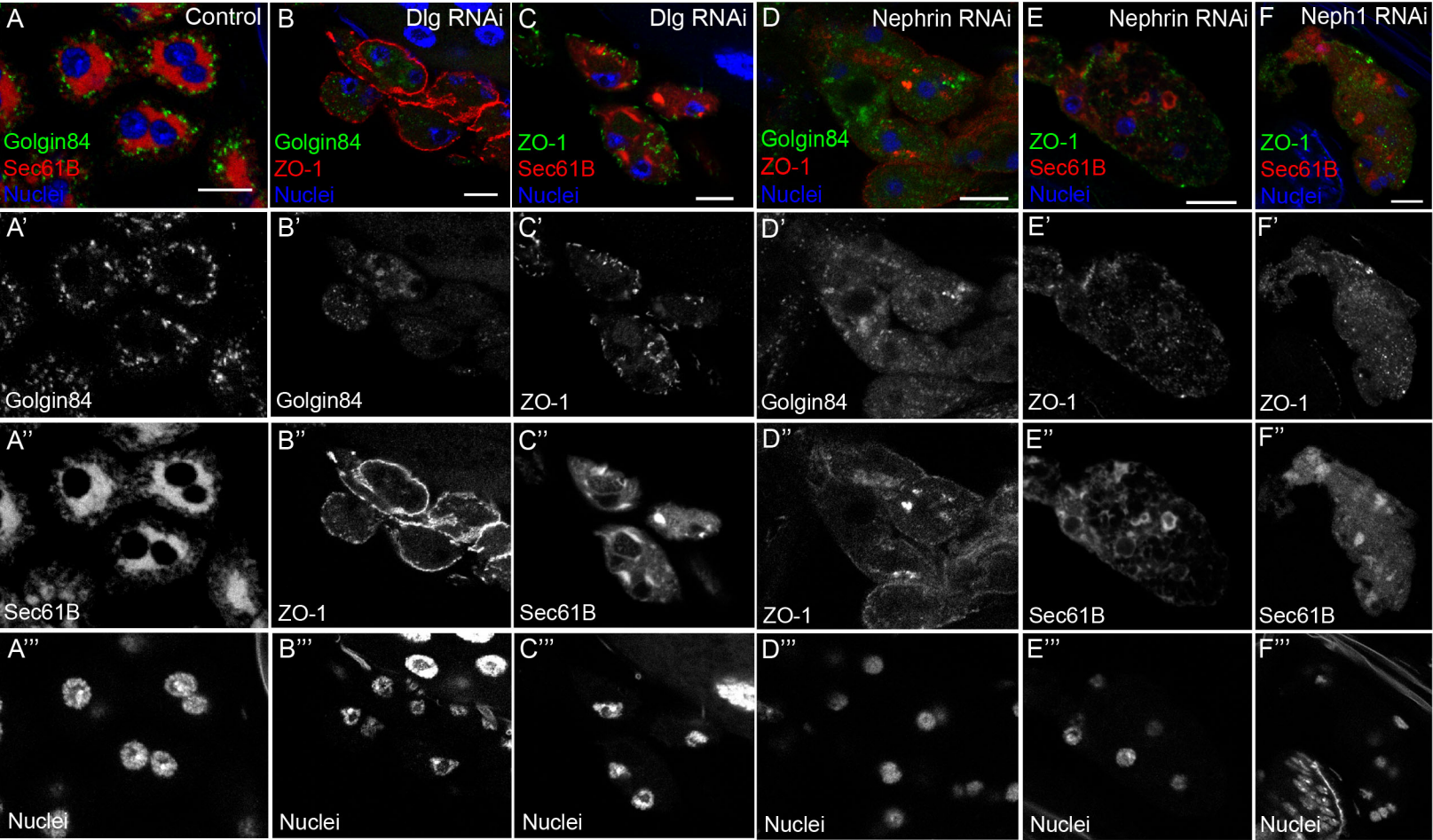
Suppl.Fig.3



Suppl.Fig.4

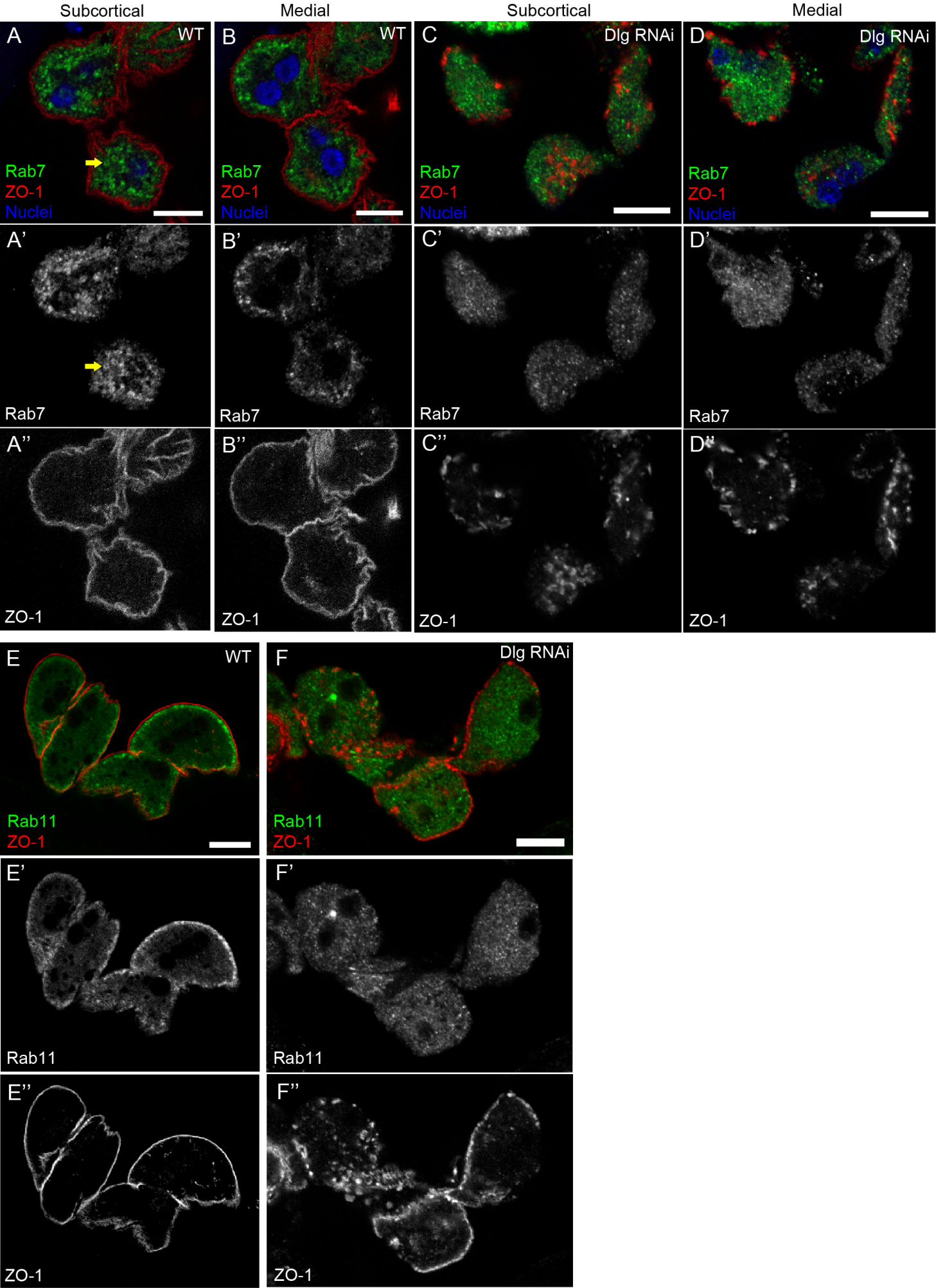


Suppl.Fig.5



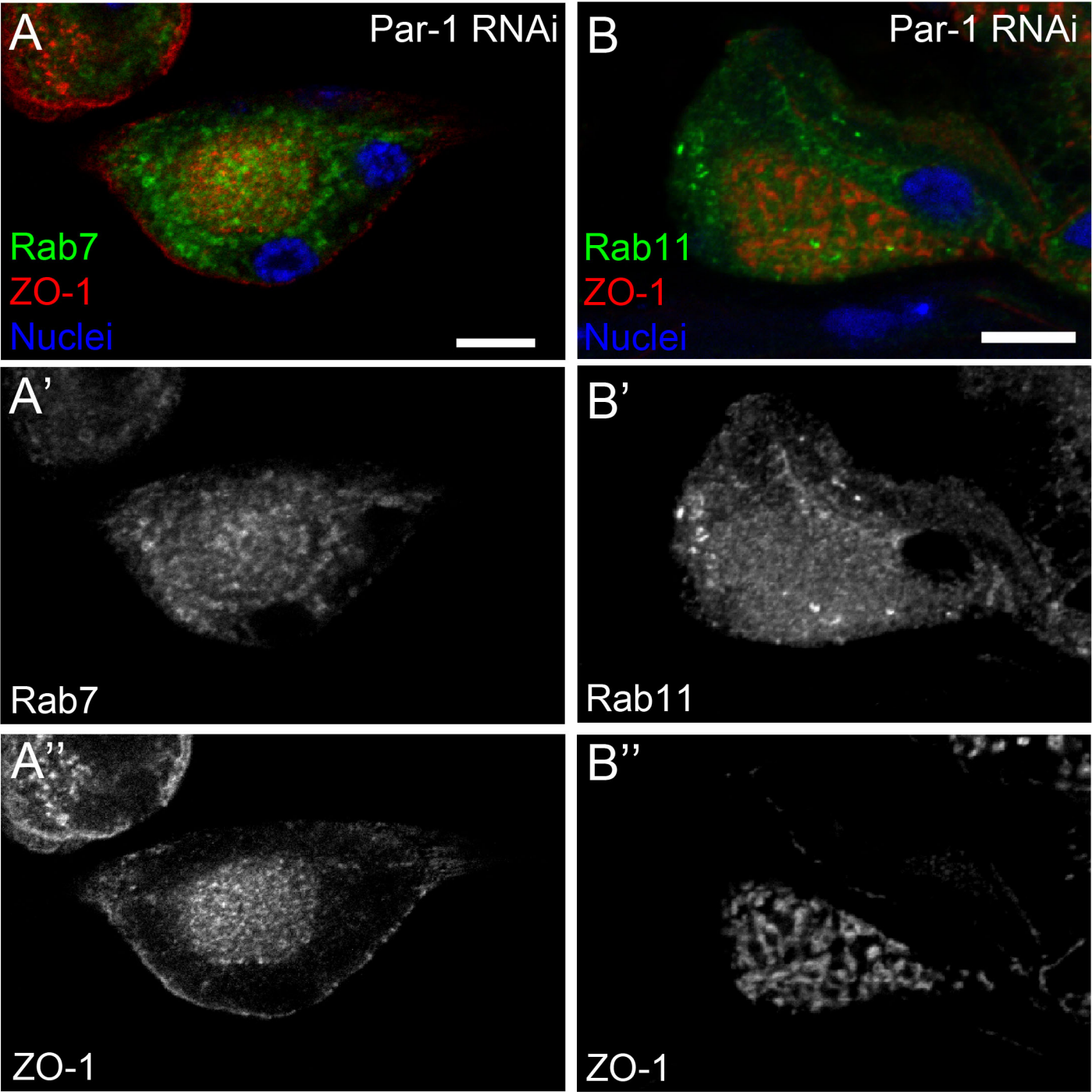


Suppl.Fig.6

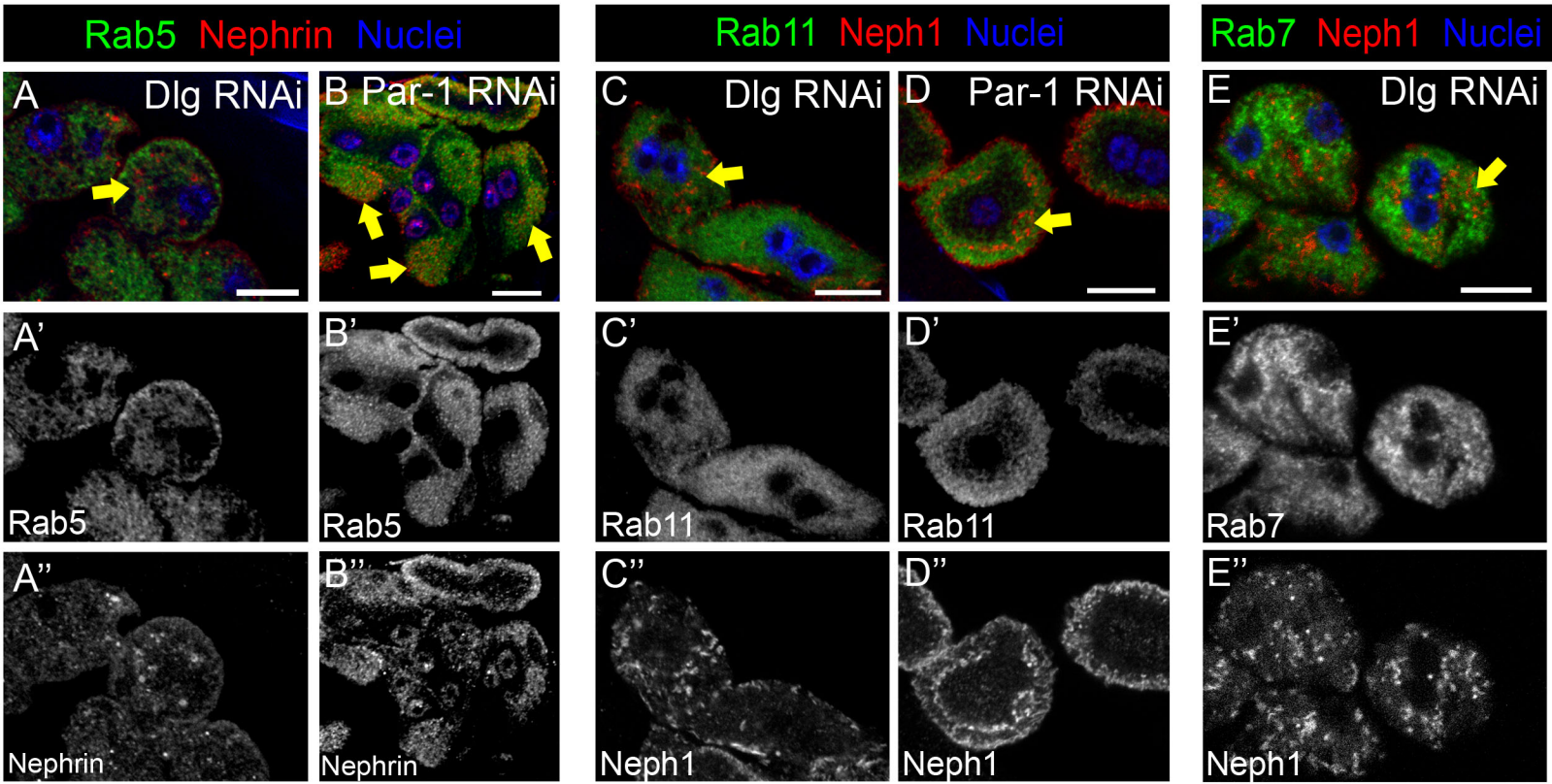




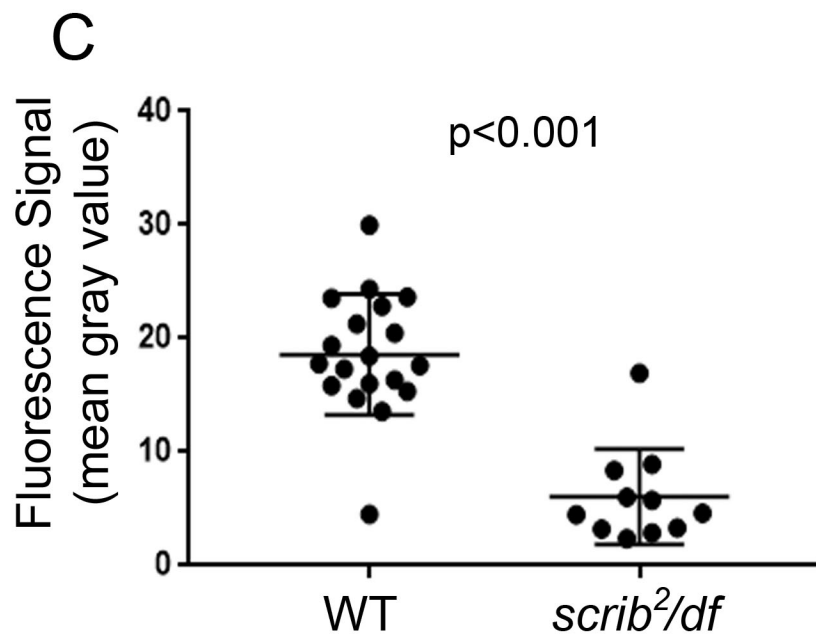
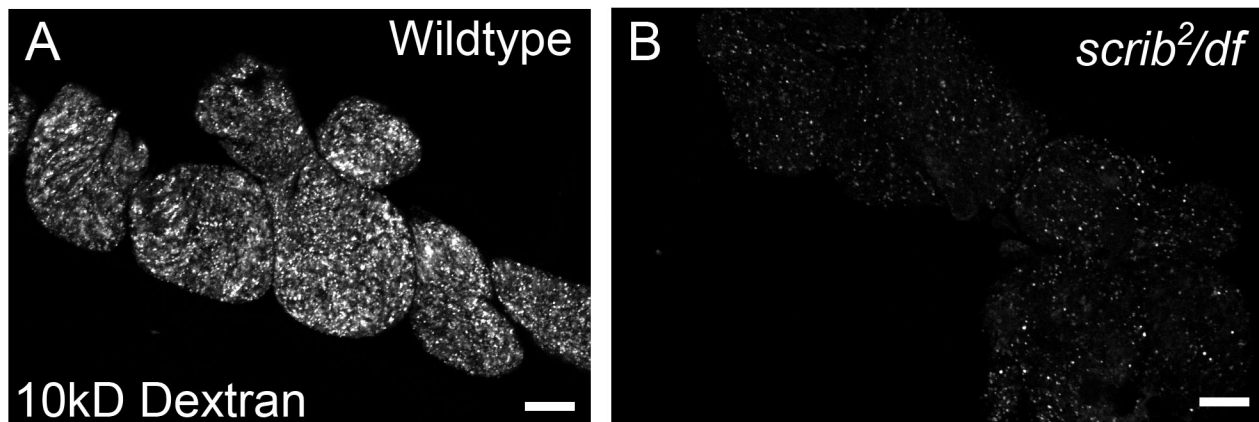
Suppl.Fig.7



Suppl.Fig.8



Suppl.Fig.9



**Suppl Table 1. List of antibodies used in this study**

<u>Antigen</u>	<u>Antibody info/clone</u>	<u>Animal</u>	<u>Dilution</u>	<u>Source</u>
ZO-1/Pyd	PYD2	Mouse	1:500	DSHB
Dlg	4F3	Mouse	1:50	DSHB
Golgin84	12-1	Mouse	1:40	DSHB
Lgl	98260	Rabbit	1:200	Santa Cruz
Scrib		Guinea Pig	1:500	David Bilder
Par-1		Guinea Pig	1:800	Denise Montell
Crb	ex3	Rat	1:1000	Elixabeth Knust
Rab5		Guinea Pig	1:2000	Akira Nakamura
Rab7		Rabbit	1:1000	Akira Nakamura
Rab11		Rabbit	1:1000	Akira Nakamura
Nephrin/Sns		Rabbit	1:1000	Susan Abmayr
Neph1/Duf		Guinea Pig	1:1000	Susan Abmayr

DSHB = Developmental Studies Hybridoma Bank